



Optimising the Formulation and Properties of UHPC Material Based on Andreasen's Model

Zhaosheng Feng^{1,a}, Wei Huang^{1,b}, Haiao Zheng^{2,c*}, and Wen Liu^{3,d}

¹The First Construction Company of CCCC Second Harbor Engineering Co. Ltd., Wuhan, Hubei, 430056, China

²School of Civil and Hydraulic Engineering, Huazhong University of Science and Technology, Wuhan, Hubei, 430074, China

³CCCC Wuhan ZhiXing International Engineering Consulting Co., Ltd., Wuhan, Hubei, 430014, China

^aerma7755@163.com, ^b375065678@qq.com
^{c*}2205233816@qq.com, ^d379047775@qq.com

Abstract. Ultra-High-Performance Concrete (UHPC) is widely utilized in the construction of critical structures due to its exceptional performance. Among its variations, RPC-type UHPC demonstrates robust mechanical and operational capabilities, but its high viscosity often necessitates its use in prefabricated components. Conversely, low-viscosity UHPC, characterized by its favourable flowability, is well-suited for on-site pouring. To enhance the performance of UHPC and develop low-viscosity formulations suitable for on-site pouring, the Andreasen model is employed for UHPC mix design, and the optimal mix ratio is determined through controlled experiments. Simultaneously, research is conducted to reduce the viscosity of UHPC through three approaches: optimizing the water to binder ratio, developing low-viscosity water-reducing agents, and utilizing shaped spherical aggregate particles. The experimental findings revealed that the optimal mix ratio for UHPC, providing its best performance, consists of 0.17 of the water to binder ratio, 840 kg/m³ of the cement, 187 kg/m³ of the silica fume, 93 kg/m³ of the fly ash, 1120 kg/m³ of the quartz sand, 157 kg/m³ of the steel fibres, and 7.1 kg/m³ of the water-reducing agent (45% solid content, 1.4% liquid content). Homemade nano-scale admixtures, shaped quartz sand aggregate, and specialized low-viscosity water-reducing agents notably reduce the viscosity of UHPC, with the homemade water-reducing agent exhibiting the most effective viscosity reduction. The prepared low-viscosity UHPC demonstrates working performance on par with C50 self-compacting concrete, achieving a compressive strength exceeding 120 MPa at 28 days, a flexural strength of over 20 MPa, and an elastic modulus surpassing 40 GPa. These research findings can serve as a valuable reference for the formulation and optimization of UHPC.

Keywords: Ultra-high performance concrete; Andreasen model; Mixing ratio design; Viscosity reduction optimisation.

1 Introduction

Since the 1990s, UHPC has garnered significant research attention. With compressive strength ranging from 3 to 10 times that of traditional concrete and a chloride ion diffusion coefficient of only 0.1%, UHPC demonstrates marked superiority over ordinary concrete. Its exceptional mechanical performance and durability have facilitated widespread applications in large-span bridges, ultra-large hydropower stations, nuclear power plants, and iconic buildings, thus underscoring its substantial potential and value in engineering construction.

The preparation of UHPC currently focuses on reducing micro-defects in cementitious materials and enhancing material compactness through optimizing pore structure and decreasing porosity. Improving overall homogeneity is crucial in minimizing micro-defects in cementitious materials, with extensive research conducted by scholars globally. Wang et al. [1] examined the phenomenon of steel fibre clustering in UHPC preparation based on the mix ratio and observed that at slump expansions of 414, 405, and 400 mm, the steel fibres did not cluster. Liang et al. [2] utilized an equal amount of ultrafine quartz powder as a replacement for cement and observed its capability to enhance UHPC homogeneity, with uniform distribution of steel fibres and good homogeneity achieved at substitution levels of 10% to 15%. Gong et al. [3] investigated the impact of water to binder ratio and fly ash additives on the workability and early mechanical properties of UHPC, demonstrating that a lower water to binder ratio can enhance mixture uniformity. In terms of porosity reduction, Liu et al. [4] used water absorption rate and SEM to analyse changes in hydration products and pore structure of UHPC, revealing a significant increase in internal pores when the water to binder ratio reached 0.19 to 0.20, with higher water to binder ratios leading to increased porosity. Xiao et al. [5] described the process of pore structure formation, influencing factors, regulatory mechanisms, and their effects on the macroscopic properties of concrete, and also summarised methods of pore structure modification, including carbonation modification, microbial modification, polymer and mineral modification. According to Golewski and Gil [6], the fracture toughness of concrete with fly ash and silica fume additives was investigated. The study found that the early fracture toughness of the material was significantly increased by applying silica fume to fly ash concrete. For the first 28 days of concrete curing, it is recommended to replace 10% of the cement with silica fume or to use a combination of additives in a 10% silica fume + 10% fly ash ratio. Mayhoub et al. [7] researched the effects of ingredients on the properties of RPC, presenting the impact of utilizing various proportions of RPC and substitutes on compressive strength under different curing regimes. The high viscosity of UHPC renders it unsuitable for on-site pouring, prompting extensive scholarly efforts to mitigate this characteristic. Khayat et al. [8] provided an overview of the rheological properties, applicable flow models, and measurement techniques of UHPC, showcasing the influence of different component materials on its rheological properties. Yahia [9] evaluated the rheological behaviour of UHPC, identifying a nonlinear relationship between viscosity and applied shear rate. E. Nguyen Amanjean et al. [10] found that metakaolin increases the viscosity and thixotropy of a given fibre concrete.

The aforementioned research has primarily focused on optimizing the UHPC preparation process, material ratios, and other factors from various perspectives, while giving less consideration to the overall aspects. The performance of UHPC is influenced by multiple factors collectively. In this study, factors such as water to binder ratio, sand to binder ratio, silica fume content, fly ash content, etc., are comprehensively considered. Experiments are conducted to investigate the optimal mix ratio for UHPC and analyse the mechanical properties under different mix ratios. Moreover, in order to broaden the application of UHPC and improve its suitability for on-site pouring, the viscosity is also optimized.

2 UHPC development test

2.1 Test material

The experiment employed P.II52.5R and P.O42.5 cements, with specific surface areas of 365.4 m²/kg and 367.6 m²/kg, respectively. Silica fume and nano-grade ultrafine powder were used as mineral admixtures, with the specific surface area of silica fume being 21400 m²/kg, and the chemical composition is detailed in Table 1. The nano-grade ultrafine powder exhibited 0% residue when sieved at 45mm. Quartz sand within the range of 0.15mm to 0.60mm was utilized as the fine aggregate, possessing a compacted bulk density of 1872 kg/m³. The admixtures included BASF 410, Sika PC-7, and a custom-made UHPC-specific polycarboxylate superplasticizer, with their performance indicators presented in Table 2. Two types of steel fibres were used: cold-drawn copper-coated fine steel fibres with lengths ranging from 6 to 14mm, and a tensile strength of 2850MPa; and hooked-end steel fibres with a length of 22mm and a tensile strength of 1000MPa. Clean tap water was used for mixing, ensuring suitability for practical engineering applications.

Table 1. Silica fume chemical composition (w/%).

Name	SiO ₂	Fe ₂ O ₃	Al ₂ O ₃	CaO	MgO
Silica fume	93.72	0.19	0.24	0.96	0.94

Table 2. Performance index of admixture.

Name	Solid content/%	PH	Water reduction rate /%
410	20	5.9	>28
PC-7	45	3.7	>31
Homemade	33	5.6	>30

2.2 Material formulation and optimization

Prior to the commencement of the experiment, the fundamental concrete mix proportion was determined using the Andreasen model. This model, underpinned by the principle of continuous grading, necessitates a uniform particle size distribution from the

smallest to the largest particles to facilitate dense packing and minimize voids. The continuous grading system is assumed to commence from infinitesimal and can be mathematically represented by the following formula:

$$U(D_p) = 100 \left(\frac{D_p}{D_{pl}} \right)^q \quad (1)$$

where, D_p represents the given particle diameter, D_{pl} represents the maximum particle diameter, $U(D_p)$ represents the volume fraction of particles smaller than D_p , and q denotes the Fuller index, which is set at 0.25.

The standard proportion of the UHPC base mix is determined through calculations, with the ratio of cement to silica fume to quartz sand to polycarboxylate superplasticizer being 1:0.2:1:0.07 and a water to binder ratio of 0.18. The standard mix proportions for RPC and low-viscosity UHPC with initial cement mixtures of 933 kg/m³ and 672 kg/m³ are detailed in Table 3.

Table 3. Base mixing ratio for UHPC type RPC (kg/m³).

Type	C	SF	FA	QS	WRSC	SF	W
RPC	933	187	-	1120	13.4	157	201.6
Low viscosity	672	112	336	1120	-	157	200

2.2.1 RPC type UHPC optimization

The study systematically investigated the impact of the water to binder ratio (R1~R4), the sand to binder ratio (R5~R8), the content of mineral admixtures (silica fume R9~R12, fly ash R13~R16), the content of chemical admixtures (R17~R20), and the content of steel fibres (R21~R24) on the workability and mechanical properties of UHPC based on the standard mix ratio.

The water to binder ratio was identified as the primary factor influencing strength, as excessive amounts lead to increased concrete porosity and reduced strength, while insufficient amounts affect workability. Notably, fine aggregate sand plays a critical role in the flowability of the RPC-type UHPC and the strength of specimens. Silica fume exhibited beneficial filling, pozzolanic, and morphological effects, while fly ash contributed to enhancing concrete workability. Additionally, though micro steel fibers effectively improved toughness and ductility, they concurrently reduced the mixture's flowability. To determine the optimal content for each factor, four sets of experiments were conducted, and the mix ratio information is detailed in Table 4.

Table 4. RPC-type optimized test mix information.

S.No.	C	SF	QS	SF	W	WRSC
R1	933	187	1120	157	190.4	13.4
R2	933	187	1120	157	212.8	13.4
R3	933	187	1120	157	235.2	13.4
R4	933	187	1120	157	257.6	13.4
R5	884	177	1179	157	201.6	13.4

S.No.	C	SF	QS	SF	W	WRSC
R6	933	187	1120	157	212.8	13.4
R7	977.5	195.5	1067	157	222.9	13.4
R8	1018	204	1018	157	232.2	13.4
R9	1018	102	1120	157	201.6	13.4
R10	974	146	1120	157	201.6	13.4
R11	933	187	1120	157	201.6	13.4
R12	896	224	1120	157	201.6	13.4
R13	1011.8	159.4	1018.2	157	232.1	13.4
R14	965.8	159.4	1018.2	157	232.1	13.4
R15	923.8	159.4	1018.2	157	232.1	13.4
R16	885.3	159.4	1018.2	157	232.1	13.4
R17	933	187	1120	157	201.6	56
R18	933	187	1120	157	201.6	67.2
R19	933	187	1120	157	201.6	78.4
R20	933	187	1120	157	201.6	89.6
R21	933	187	1120	0	201.6	13.4
R22	933	187	1120	78.5	201.6	13.4
R23	933	187	1120	157	201.6	13.4
R24	933	187	1120	235.5	201.6	13.4

2.2.2 Low viscosity optimization

The traditional RPC-type UHPC exhibits significant shortcomings in the construction of cast-in-place structures and pump operations due to its high viscosity and limited flowability. There are currently three methods for reducing viscosity: decreasing the amount of binding material and increasing water content, developing low-viscosity water-reducing agents, and utilizing shaped ball-like aggregates. In light of this, a controlled experiment was established to investigate the influence of viscosity and mechanical properties of UHPC during the preparation process on the content of viscosity-reducing water-reducing agent, cementitious materials, shaped quartz sand, and water usage. The contents of the water-reducing agent in the four experimental groups (R25~R28) were 1.5%, 2.0%, 2.5%, and 3.0% respectively, using the dedicated water-reducing agent content as the research variable. Moreover, for the cementitious materials (R29~R32), a self-developed nano-cementitious admixture was employed to replace fly ash at replacement ratios of 40%, 60%, 80%, and 100%. Additionally, a control experiment was conducted for the shaped quartz sand (R33~R34), comparing ordinary quartz sand with shaped quartz sand particles. Water to binder ratios of 0.16, 0.18, and 0.2 were utilized for various performance tests in relation to water usage (R35~R37). The baseline mix proportions for each group of experiments are detailed in Table 5.

Table 5. Low viscosity optimized test reference ratios(kg/m³).

RO.	C	SF	FA	QS	SF	W	WRSC	MNA
R25~R28	672	112	336	1120	157	200	-	-
R29~R32	6723	1127	336	1120	157	200	22.4	-
R33~R34	672	112	-	1120	157	200	22.4	336
R35~R37	672	112	-	1120	157	-	22.4	336

2.3 Specimen Preparation and Test Methods

In the production of UHPC, the mixing process begins with the addition of dry materials, followed by mixing at medium to low speed in the mixer for 1 to 2 minutes to ensure uniform blending. Water is then slowly added to the mixture and stirred for 3 minutes, followed by rapid stirring for 5 minutes to promote thorough mixing of the raw materials, water, and water-reducing agent. Subsequently, steel fibres are added, and the mixture is stirred at low speed before stopping. The resulting slurry is poured into a 100mm×100mm×100mm standard mould and left to cure in air at 20°C until the specified age is reached.

Following the guidelines set out in the GB/T 50080-2002 "Standard Test Method for Performance of Ordinary Concrete Mixtures," the slump is assessed using a cone-shaped mould, and the spread is assessed utilizing a concrete flow test bench. Mechanical properties, such as compressive strength, are evaluated in accordance with the standards defined in GB/T 50081-2002 "Standard Test Method for Mechanical Properties of Ordinary Concrete," using a computer-controlled electronic universal testing machine.

3 Analysis of test results

3.1 Analysis of RPC-type UHPC optimization test results

The results of the water to binder ratio test for RPC-type UHPC are depicted in Fig.1. Both the slump and spread increase gradually with the elevation of the water to binder ratio, reaching their peak values after 28 days, with a strength of 108.1 MPa. This occurrence is attributed to the limited flowability of the mixture at lower water to binder ratios, exacerbated by the high-water demand of the silica fume, resulting in a significant reduction of available free water for hydration within the system. Consequently, the viscosity of RPC-type UHPC rises, impeding the release of air bubbles, impacting the compaction and formation of the mixture, and leading to a reduction in strength. As the water to binder ratio continues to increase, the flowability of the mixture improves, ultimately enhancing the overall performance of UHPC. It is important to note that beyond a water to binder ratio of 0.23, it becomes the primary determinant of RPC-type UHPC strength, and excessively high ratios can lead to a strength decrease.

As the sand to binder ratio increases, the quantity of cementitious materials increases, leading to the enhancement of both the workability and mechanical performance of RPC-type UHPC. Fig.2 illustrates that at a sand to binder ratio of 1.2, the

compressive strength peaks at 111.3 MPa after 28 days. The augmented sand to binder ratio raises the proportion of cementitious materials, consequently increasing the volume of the paste surrounding the fine aggregates, thereby improving the flowability of the RPC-type UHPC mixture. Simultaneously, the cementitious materials contribute to a more compact UHPC structure, resulting in increased strength.

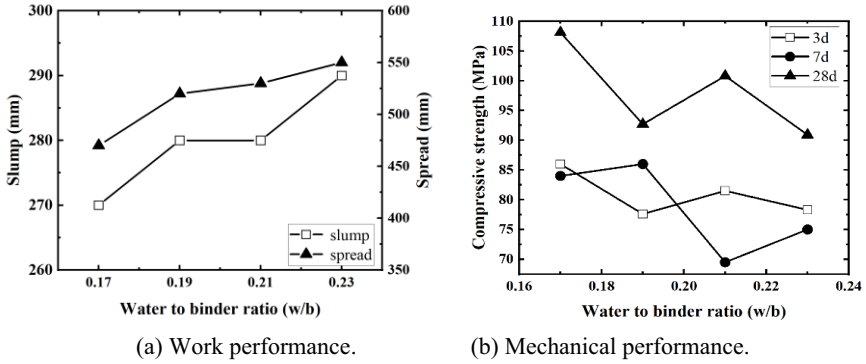


Fig. 1. Water to binder ratio test results.

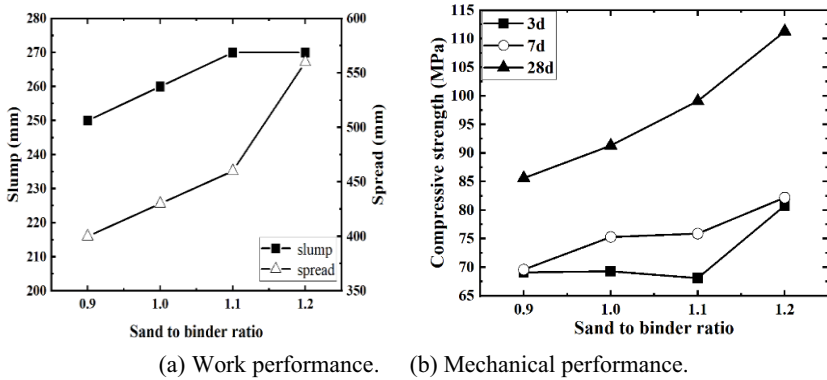
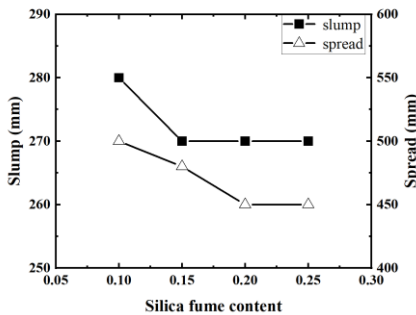
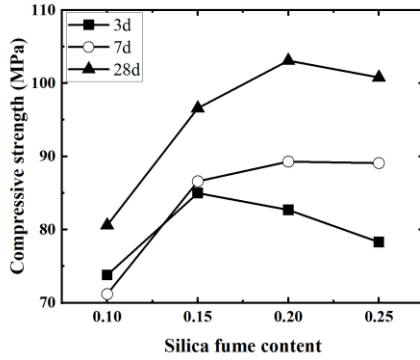


Fig. 2. Sand to binder ratio test results.

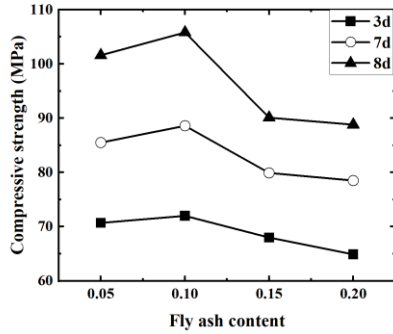
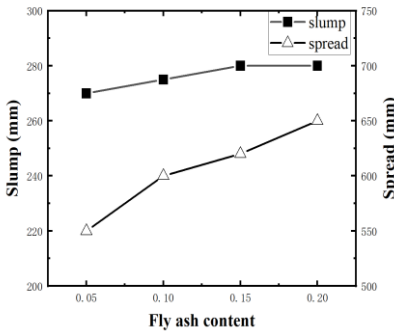


(a) Work performance.



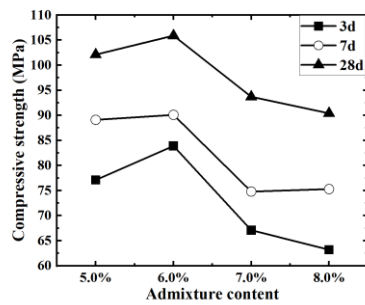
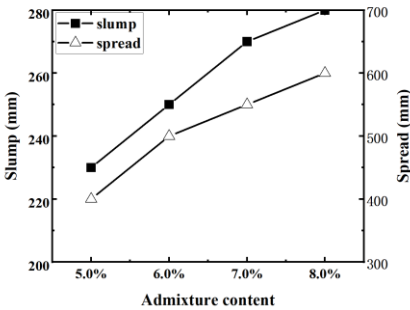
(b) Mechanical performance.

Fig. 3. Silica fume content test results.



(a) Work performance. (b) Mechanical performance.

Fig. 4. Fly ash content test results.



(a) Work performance. (b) Mechanical performance.

Fig. 5. Admixture content test results.

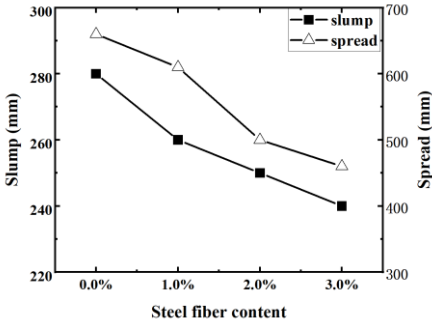
The workability of RPC-type UHPC mixtures decreases as the silica fume content increases. This can be attributed to the fine particles, large specific surface area, and

high-water demand of silica fume. Consequently, as the silica fume content increases, the amount of encapsulated water also increases, leading to a reduction in the workability of the mixture. This relationship is illustrated in Fig.3, which demonstrates a significant effect of silica fume content on the strength of RPC-type UHPC, showcasing an initial increase followed by a decrease, with the highest strength being 103.1MPa. The theory of dense packing of particles indicates that silica fume can fill the voids among cement particles and promote densification. Specifically, a low amount of silica fume can improve the compactness of the system, thereby enhancing its strength. Conversely, a high amount of silica fume causes a decrease in the flowability of the mixture, due to the large specific surface area of silica fume, resulting in increased viscosity and the difficulty of releasing internal air bubbles, thus reducing the strength of UHPC. In conclusion, it is advisable for the amount of silica fume to be 20% of the amount of cement.

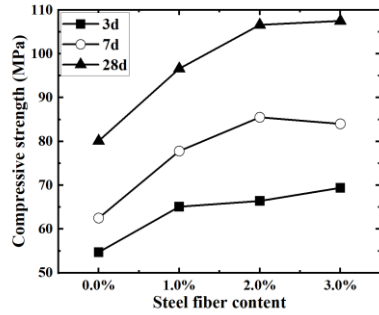
The influence of fly ash content on the workability and mechanical performance of RPC-type UHPC mixture is evident from the test results depicted in Fig.4. As the fly ash content increases, there is a notable enhancement in the workability of the RPC-type UHPC mixture, with a maximum spread of 650mm achieved and a noticeable reduction in viscosity. Specifically, at a fly ash content of 0.1, the RPC-type UHPC exhibits its highest strength, reaching 105.8MPa. The filling effect of fly ash and its secondary pozzolanic impact contribute to the mitigation of internal micro-cracks, thereby enhancing later strength. It's important to note that exceeding a certain value in the replacement of cement content with fly ash leads to decreased strength due to its low activity and poor filling ability. Notably, a comprehensive analysis reveals that the optimal effect is observed when the fly ash content accounts for 10% of the cement.

Fig.5 illustrates the impact of admixture content on the performance of RPC-type UHPC. Increased admixture content substantially enhances the workability of UHPC. However, it also leads to a higher gas content within the system. This increased gas content, while improving flowability, reduces the compactness of the resulting mixture, resulting in a slight initial increase followed by a gradual decrease in compressive strength. Consequently, the preparation of RPC-type UHPC is deemed appropriate with a 6% water-reducing agent content.

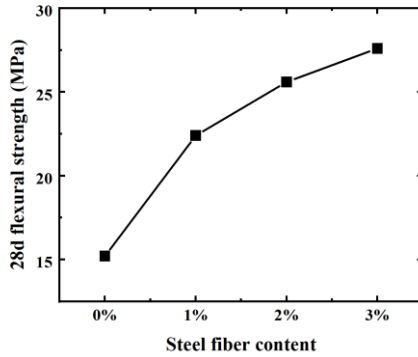
The paper delves into the substantial impact of steel fibre content on the mechanical properties of RPC-type UHPC. With an increase in steel fibre content, the workability of UHPC decreases, leading to decreased slump and spread, and increased concrete viscosity, as depicted in Fig.6(a). In Fig.6(b) and Fig.6(c), both compressive and flexural strengths demonstrate a gradual increase, culminating in a maximum compressive strength of 107.5 MPa and a flexural strength of 27.5 MPa. Fine steel fibres have the capacity to augment the toughness of RPC-type UHPC, mitigate brittleness, and fortify both its compressive and flexural strengths. However, an excessively high steel fibre content escalates costs and diminishes workability. Considering workability, strength, and cost-efficiency, a steel fibre volume content of 2% emerges as the most suitable option.



(a) Work performance.



(b) Compressive strength.



(c) Flexural strength.

Fig. 6. Steel fibre content test results.

3.2 Analysis of low viscosity optimization test results

3.2.1 Mixing ratio optimization test

Table 6 presents the experimental findings regarding the influence of a specialized water-reducing agent on UHPC. As the content of the water-reducing agent increases, the flowability of UHPC mixtures improves and the viscosity decreases. Specifically, the specialized low-viscosity water-reducing agent boosts adsorption and dispersion, induces electrostatic repulsion among cement particles, disrupts the flocculation structure of the mixture, releases bound water, and augments the water film thickness, thereby reducing the viscosity. However, the reduction in viscosity weakens with an increase in the content of the water-reducing agent. Regarding compressive strength, the increase in the content of the water-reducing agent from 1.5% to 3.0% results in a decrease in the 28-day compressive strength from 135 MPa to 132 MPa, while the flexural strength and elastic modulus remain stable.

Table 6. Specialized water reducing agent content test data.

WRAC (%)	Fluidity (mm)	Viscosity (Pa·S)	28d CS (MPa)	28d FS (MPa)	EM (GPa)
1.5	400	20.15	135	26.5	48.0
2.0	500	16.23	134.5	26.4	48.2
2.5	600	11.34	132.4	26.6	48.1
3.0	650	10.15	132.0	26.3	48.0

As the proportion of in-house produced micro-nano admixtures increases, the flowability of UHPC mixtures improves, and the viscosity notably decreases, as documented in Table 7. The diminutive particle size and extensive specific surface area of the micro-nano admixtures augment inter-particle dispersion, diminish friction, and effectively reduce the overall viscosity of the mixtures. This effect amplifies with rising admixture ratios. The compressive strength of UHPC steadily rises in tandem with the replacement ratio. The incorporation of admixtures enhances the density and uniformity of the mixtures, subsequently fortifying the microstructure of UHPC and enhancing its mechanical properties. Nonetheless, their impact on the flexural strength and elastic modulus of UHPC is constrained, as these properties are significantly influenced by the macrostructure and long-term performance changes of the material, rather than being governed solely by the microscopic adjustment of particle size and distribution.

Table 7. Micro and nano dopant test data.

FA Substitution (%)	Fluidity (mm)	Viscosity (Pa·S)	28d CS (MPa)	28d FS (MPa)	EM (GPa)
40	520	135	26.7	48.5	135
60	550	137.5	26.5	48.8	137.5
80	580	142.4	26.6	48.3	142.4
100	600	146.5	26.7	48.6	146.5

Substituting ordinary quartz sand with particle-shaped quartz sand enhances the flowability of UHPC mixtures and significantly reduces viscosity. This change is attributed to the shape and surface properties of the particle-shaped quartz sand. While ordinary quartz sand is angular and forms tight bonds with cementitious materials, resulting in higher strength, the particle-shaped quartz sand, despite improving flowability, forms less secure bonds with the cementitious materials due to its shape and surface properties, leading to a slight decrease in strength. The influence of particle-shaped quartz sand on the elastic modulus of UHPC is limited, possibly because the elastic modulus is primarily determined by the material's microstructure and composition, with the particle shape having minimal impact. The experimental results regarding the quartz sand are presented in Table 8.

Table 8. Granular shaping quartz sand test data.

Quartz Sand Types	Fluidity (mm)	Viscosity (Pa·S)	28d CS (MPa)	28d FS (MPa)	EM (GPa)
OQS	600	146.5	26.7	48.6	146.5
PSQS	640	145.5	26.0	48.8	145.5

Table 9. Water to binder ratio test data.

W/B	Spreadability (mm)	Viscosity (Pa·S)	28d CS (MPa)	28d FS (MPa)	EM (GPa)
1.5	550	14.0	148.5	26.7	48.6
2.0	640	11.03	145.5	26.0	48.8
2.5	750	9.3	136.2	25.8	48.6
3.0	550	14.0	148.5	26.7	48.6

Table 9 illustrates the test results regarding the water to binder ratio. As the water to binder ratio increases, the workability of UHPC mixtures improves and the viscosity decreases. Furthermore, a higher water to binder ratio leads to the release of more free water, resulting in enhanced lubrication of the UHPC paste. However, the higher water content contributes to increased porosity within the concrete, leading to reduced structural density, load-bearing capacity, and a slight decrease in compressive strength. It is worth noting that the water to binder ratio has a relatively minor impact on flexural strength and elastic modulus, as these properties depend on the material's microstructure and the effect of fibre reinforcement, rather than being solely influenced by the water to binder ratio.

3.2.2 Viscosity reduction effect analysis

The performance of low-viscosity UHPC is compared with that of typical C50 self-compacting concrete, as depicted in Table 10 to ascertain the effect of viscosity reduction. Upon the addition of a specialized water reducer, the workability of UHPC improves and its viscosity decreases. Using the self-compacting concrete assessment method, the V-funnel time is recorded at 7.4 seconds, and the T500 time at 9.0 seconds, both equivalent to those of ordinary C50 self-compacting concrete. Although the viscosity of standard UHPC generally exceeds that of high-strength concrete, the viscosity of this low-viscosity UHPC adheres to the standard of typical self-compacting concrete, indicating the successful implementation of the viscosity reduction method.

Table 10. Comparison of low viscosity UHPC and C50 self-compacting concrete performance.

CT	Spreadability (mm)	Viscosity (Pa·S)	V75 Funnel Time(S)	T500(S)
LV-UHPC	700	9.2	7.4	8.8
C50-SCC	620	10.6	7.5	9.0

4 Conclusion

To enhance the mechanical properties and workability of UHPC, a comparative experimental study was conducted to explore the impact of various materials, and a mix design was developed using the Andreasen model. By focusing on three approaches—reducing the amount of binder, increasing water content, and developing a low-viscosity water reducer—an optimization of low-viscosity UHPC was carried out. The main conclusions are as follows:

(1) The preferred materials for preparing UHPC are P.O 42.5 cement, high-quality silica fume, fly ash beads, high-quality quartz sand, 12mm fine steel fibres, and a high efficiency polycarboxylate superplasticizer. The optimal mix design includes a water to binder ratio of 0.17, comprised of 840kg/m³ of cement, 187kg/m³ of silica fume, 93kg/m³ of fly ash, 1120kg/m³ of quartz sand, 157kg/m³ of steel fibres, and 7.1kg/m³ of water reducer (45% solid content, 1.4% solution content).

(2) Low-viscosity UHPC was achieved by using homemade micro-nano admixtures, particle-shaped quartz sand, and a specialized low-viscosity water reducer. The homemade water reducer had the most significant effect on viscosity reduction, followed by the particle-shaped quartz sand, while the micro-nano admixture had a relatively weaker effect. The resulting low-viscosity UHPC demonstrated equivalent workability to C50 self-compacting concrete, meeting the standards for self-compacting concrete. Moreover, the low-viscosity UHPC exhibited outstanding mechanical performance after hardening, with compressive strength exceeding 120MPa, flexural strength surpassing 20MPa, and elastic modulus exceeding 40GPa. The optimal mix design comprised 672kg/m³ of cement, 112kg/m³ of silica fume, 336kg/m³ of micro-nano admixture, 1120kg/m³ of particle-shaped quartz sand, 157kg/m³ of steel fibres, 28kg/m³ of water reducer (30% solid content), and water content of 200g/m³.

(3) Maintaining low viscosity while ensuring homogeneity and stability is a critical challenge in UHPC development and a crucial focus of future research. This encompasses precise control over the selection and proportioning of raw materials, as well as the mixing process and curing mechanism. As a result, future research on UHPC performance optimization will emphasize the development of new chemical additives and enhancements to existing UHPC preparation techniques.

References

1. Wang, Z.J., Zhang, Y. and Xie, E.H. (2023) Study on uniformity control of coarse aggregate UHPC and its application in long span bridges. *Concrete*, vol. 2, pp. 186-192. <https://doi.org/10.3969/j.issn.1002-3550.2023.02.040>.
2. Liang, Y.B. and Wang, C.Q. (2021) Effect of ultrafine quartz powder on bridge deck UHPC properties. *Concrete*. vol. 5, pp. 13-15+22. <https://doi.org/10.3969/j.issn.1002-3550.2021.05.004>.
3. Gong, Z.Y., Gu, B.W., Zou, J.L. and Chen, D.Y. (2022) Study on early performance of UHPC with different mix proportions. *New Building Materials*, 49: 27-30+35. <https://doi.org/10.3969/j.issn.1001-702X.2022.12.006>.

4. Liu, C.X., Du, S., Gao, Z.H., Yu, L.Y. and Zhou, Z.H. (2023) Investigation on the impact of water-binder ratio on UHPC strength development and microstructure evolution, *Concrete*, vol. 7, pp. 39-43. <https://doi.org/10.3969/j.issn.1002-3550.2023.07.009>.
5. Xiao, J.Z., Lv, Z.Y., Duan Z.H., and Zhang, C.Z. (2023) Pore structure characteristics, modulation and its effect on concrete properties: A review. *Construction and Building Materials* 397: 132430. <https://doi.org/10.1016/j.conbuildmat.2023.132430>.
6. Golewski, G.L., and Gil, D.M. (2021) Studies of Fracture Toughness in Concretes Containing Fly Ash and Silica Fume in the First 28 Days of Curing. *Materials*, 14(2). <https://doi.org/10.3390/ma14020319>.
7. Mayhoub, O. A. and Nasr E.-S. A. R., Ali Y. A., and Kohail M. (2021) The influence of ingredients on the properties of reactive powder concrete: A review. *Ain Shams Engineering Journal*, 12(1): 145–158. <https://doi.org/10.1016/j.asej.2020.07.016>.
8. Khayat K.H., Meng W., Vallurupalli K., and Teng L. (2019) Rheological properties of ultra-high-performance concrete - An overview. *Cement and Concrete Research*, vol. 124, pp. 105828. <https://doi.org/10.1016/j.cemconres.2019.105828>.
9. Yahia A. (2011) Shear-thickening behavior of high-performance cement grouts - Influencing mix-design parameters. *Cement and Concrete Research*, 41(3): 230-235. <https://doi.org/10.1016/j.cemconres.2010.11.004>.
10. Nguyen Amanjean, E., Mouret, M., and Vidal, T. (2019) Effect of design parameters on the properties of ultra-high performance fibre-reinforced concrete in the fresh state. *Construction and Building Materials*, 224: 1007-1017. <https://doi.org/10.1016/j.conbuildmat.2019.07.284>.

Open Access This chapter is licensed under the terms of the Creative Commons Attribution-NonCommercial 4.0 International License (<http://creativecommons.org/licenses/by-nc/4.0/>), which permits any noncommercial use, sharing, adaptation, distribution and reproduction in any medium or format, as long as you give appropriate credit to the original author(s) and the source, provide a link to the Creative Commons license and indicate if changes were made.

The images or other third party material in this chapter are included in the chapter's Creative Commons license, unless indicated otherwise in a credit line to the material. If material is not included in the chapter's Creative Commons license and your intended use is not permitted by statutory regulation or exceeds the permitted use, you will need to obtain permission directly from the copyright holder.

